RAD51 Enhances Zygotic Interhomolog Repair

Jonathan J. Wilde[1], Tomomi Aida[1], Martin Wienisch[1], Qiangge Zhang[1], Peimin Qi[1], and Guoping Feng[1,2]*

Affiliations:
[1]McGovern Institute for Brain Research, Department of Brain and Cognitive Sciences, Massachusetts Institute of Technology (MIT), Cambridge, Massachusetts 02139, USA

[2]Stanley Center for Psychiatric Research, Broad Institute of MIT and Harvard, Cambridge, Massachusetts 02142, USA

*Correspondence to G.F.: fengg@mit.edu

45   **Recent advances in CRISPR/Cas-based genome editing, including three-component**

46   **CRISPR[1], the use of long single-strand donors[2], enhanced microhomology-mediated end-**

47   **joining (MMEJ)[3], and pharmacological approaches[4-7] have greatly improved knock-in (KI)**

48   **efficiency. In our search for factors to further improve KI efficiency for broad therapeutic**

49   **use and efficient generation of primate disease models, we found that the strand exchange**

50   **protein RAD51 can significantly increase homozygous KI efficiency using CRISPR/Cas9 in**

51   **mouse embryos through an interhomolog repair (IHR) mechanism. Using a variety of**

52   **approaches, we demonstrate robust enhancement of zygotic IHR by RAD51 and show that**

53   **this can be leveraged both for generating homozygous KI animals from wildtype zygotes**

54   **with exogenous donors and for converting heterozygous alleles into homozygous alleles**

55   **without exogenous templates. Thus, our study provides both conclusive evidence**

56   **supporting the existence of zygotic IHR mechanisms and a new method to significantly**

57   **improve IHR efficiency for potential therapeutic use.**

58   We previously described a three-component CRISPR approach, which employs Cas9

59   protein and chemically synthesized crRNA and tracrRNA for efficient KI of transgenes[1,2,8].

60   Additional published work in rabbit embryos has shown significant enhancement of KI

61   efficiency using RS-1, a chemical agonist of the homology-directed repair (HDR) pathway

62   member RAD51[6]. We began our study by attempting to use a combination of these techniques

63   for high-efficiency knock-in of an autism-associated point mutation in *Chd2* (c.5051G>A;

64   R1685H in human, R1684H in mouse; hereon referred to as *Chd2[R1684H]*; **Fig. 1a**) using a single-

65   stranded oligonucleotide donor (ssODN). Previous studies have shown that KI efficiency is

66   affected by the proximity of the Cas9 cut site and the insertion site[9], so we chose a guide

67   positioned where the cut site is directly adjacent to the desired G>A point mutation. Genotyping

68   of mouse embryos after pronuclear injection and *in vitro* culture with or without RS-1 (7.5μM)

69   showed a high KI efficiency at the targeted *Chd2* locus, but revealed that RS-1 did not affect KI

70   efficiency (**Extended Data Fig. 1**). Although the known mechanisms of RAD51 function

71   suggest it may not promote knock-in with ssODNs, our previous success using exogenous

72   protein to promote high-efficiency KI[1,2,3,8] and the fact that RS-1 can be highly dosage-sensitive[6]

73   led us to hypothesize that the use of exogenous RAD51 protein in combination with three-

74   component CRISPR could potentially increase KI efficiency. We first performed both pronuclear

75   (PNI) and cytoplasmic (CPI) injections of crRNA, tracrRNA, Cas9, ssODN (30 ng/μL for PNI

76   and 100 ng/μL for CPI), and RAD51 protein in mouse zygotes and genotyped the resulting F_0

77   pups (example chromatograms in **Fig. 1b**). In 18 pups, we observed an overall KI efficiency of

78   61.1% (**Fig. 1c**) and, surprisingly, a homozygous KI efficiency of 55.5% (**Fig. 1d**). We did not

79   observe significant differences in efficiency between CPI and PNI (**Extended Data Fig. 2**), so

80   we focused on PNI for the remainder of this study. Although we performed all genotyping of

81   these animals using primers sitting outside of the homology arms, we could not rule out the

82   possibility that the homozygous animals were actually compound heterozygotes with large

83   deletions encompassing the cut site on one allele[10]. We therefore bred 6 of the F_0 homozygous

84   KI mice with wildtype C57BL/6N animals and genotyped the resulting F_1 progeny. Sanger

85   sequencing showed that all 36 F_1 pups were heterozygous mutants, confirming the homozygosity

86   of F_0 animals (**Fig. 1e**).

87   Since we did not initially generate *Chd2[R1684H]* mice with injections lacking RAD51, we

88   performed additional injections to directly assess the ability of RAD51 to increase KI efficiency.

89   Zygotic injections were performed with and without RAD51, embryos were cultured for two

90   days, and nested PCR was performed for genotyping. Sanger sequencing revealed that RAD51

91   only slightly increased overall KI efficiency (**Fig. 2a**, left, p<0.05, one-tailed chi-square test), but

92   drastically increased homozygous KI efficiency (**Fig. 2a, right**, p<0.0001, one-tailed chi-square

93   test). It is widely accepted that CRISPR/Cas9-mediated editing efficiency can be highly locus-

94   and guide-dependent, so we investigated the effects of RAD51 at a second genomic locus to

95   confirm its efficacy. Using the same injection strategy employed for *Chd2*, we attempted to

96   knock in an albinism-associated human mutation (c.265T>A; C89S; hereon referred to as

97   *Tyr^{C89S}*; schematic in **Fig. 2b**) in the *Tyr* gene[11], which encodes for tyrosinase, the rate-limiting

98   enzyme in melanin production. Albinism is a recessive disorder and, as such, only homozygous

99   mutation of *Tyr* results in mice completely lacking pigment (**Fig. 2c, d**). However, indel-induced

100   disruption of *Tyr* can also result in albinism, so all F_0 animals were genotyped to assess the

101   effects of RAD51. Injections without RAD51 showed a high overall KI efficiency, but this

102   efficiency was not significantly affected by the addition of RAD51 (**Fig. 2e, left**). However, our

103   genotyping results again indicated that RAD51 can significantly increase homozygous KI

104   efficiency, with 44.4% of pups exhibiting an albino phenotype resulting from homozygous KI of

105   the *Tyr^{C89S}* allele with RAD51, as compared to only 12% without (**Fig. 2e, right**).

106   Strikingly, RAD51 co-injection more than doubled the observed homozygosity at both

107   the *Chd2* and *Tyr* loci (**Fig. 2a, e**). Previous attempts to increase HDR through pharmacological

108   or genetic mechanisms have not shown such high homozygosity rates[7,9,12], leading us to question

109   the mechanism by which RAD51 can promote such an outcome. Our evidence that RAD51 does

110   not strongly affect overall efficiency of ssODN-mediated knock-in (**Fig. 2a,d**) suggested that its

111   effects on homozygosity do not come from directly increasing independent KI events on both

112   alleles. Additionally, due to the random nature of insertion-deletions (indels) produced by non-

113   homologous end joining (NHEJ), we found it surprising that we observed multiple embryos from

114 both $Chd2^{R1684H}$ and Tyr^{C89S} injections whose genotyping results suggested the presence of the

115 same indel on both alleles (**Extended Data Fig. 3**). Genotyping of F_1 pups derived from a female

116 with such a homozygous indel revealed that all pups were heterozygous for the same indel,

117 indicating that the phenomenon was not due to an indel on one allele and a large deletion

118 encompassing the cut site on the other (**Extended Data Fig. 3**). Although we could not rule out

119 that these deletions were generated by MMEJ, which can result in stereotyped indels based on

120 local homology[3,13], the variety of observed indels suggested that the homozygosity resulted from

121 recombination between homologs that transferred the KI or indel allele from one chromosome to

122 the other.

123 More than 20 years ago, experiments in mouse ES cells found evidence of recombination

124 events between homologous chromosomes[14,15]. While these interhomolog repair (IHR) events

125 are now well-understood in meiotic cells, their occurrence in zygotes and somatic cells is poorly

126 described. However, recently published data from experiments attempting to correct a 4bp

127 GAGT deletion in *MYBPC3* in human embryos support a potential zygotic IHR mechanism

128 whereby one allele can serve as the repair template for the other after induction of a targeted

129 double-strand break (DSB) by Cas9[16]. Based on these data, we hypothesized that RAD51

130 promotes homozygous KI through a similar mechanism. To test this, we first performed PNI

131 using an injection mixture containing an equimolar ratio of two separate ssODNs containing

132 different point mutations at the same loci, allowing us to identify independent knock-in events

133 via the observation of compound heterozygosity (**Fig. 3a**). In line with our previous observations

134 (**Fig. 2a**), we found that co-injection of RAD51 significantly increased homozygous KI

135 efficiency **(Fig. 3b)**. Strikingly, compound heterozygosity was observed in 5/12 control embryos

136 with a KI event on both alleles, but was not observed in any RAD51-injected embryos (**Fig. 3b**),

137   supporting our hypothesis that RAD51 increases homozygosity through an enhanced IHR

138   mechanism. Importantly, we did not observe significant differences in overall KI rates between

139   the two ssODNs (**Extended Data Fig. 4**), ruling out the possibility that our observations were

140   due to a bias toward one donor over the other.

141   In order to more directly test the IHR mechanism, we attempted to generate homozygous

142   *Chd2^{R1684H}* embryos without the use of an exogenous donor through homozygous conversion.

143   Using *in vitro* fertilization (IVF) with wildtype C57Bl/6N eggs and sperm from homozygous

144   *Chd2^{R1684H}* male mice, we generated heterozygous zygotes and specifically targeted Cas9 to the

145   maternal *Chd2* locus. As illustrated in **Figure 3c**, PNI was performed on zygotes at ~8 hours post

146   fertilization (hpf) using a mixture of crRNA, tracrRNA, and Cas9 with or without RAD51.

147   Because the *Chd2^{R1684H}* allele contains mutations in both the guide sequence and its associated

148   PAM, Cas9 is only capable of cutting the wildtype maternal allele (**Extended Data Fig. 5**).

149   Therefore, by omitting the donor template from the injection mixture we were able to directly

150   test both the rate of baseline CRISPR/Cas9-mediated IHR in the zygote and the ability of

151   RAD51 to enhance such a mechanism. In support of data published by Ma *et al*., we observed

152   IHR events in 26% of control-injected embryos (**Fig. 3d,e**). Strikingly, co-injection of RAD51

153   was capable of increasing this rate to 74% (**Fig. 3e**). To directly rule out the possibility of false

154   positives resulting from monoallelic deletions on the maternal allele, we developed and

155   performed a genomic qPCR assay to analyze copy number at the targeted locus (**see Methods**).

156   First, using genomic DNA from wildtype mice and *Shank3B$^{+/-}$* mice harboring a heterozygous

157   deletion of exon 13 of *Shank3*[17], we confirmed that our method was capable of identifying

158   heterozygous deletions **(Fig. 3f)**. Using the same assay design, we confirmed that 5 of 5

159   randomly selected homozygous mutants carried 2 copies of the *Chd2* locus (**Fig. 3f**), validating

160   our conclusion that RAD51 enhances zygotic IHR.

161   Our data demonstrate that RAD51 enhances interhomolog repair and that this

162   enhancement can be leveraged for both donor-free homozygous conversion and *de novo*

163   homozygous KI. To our knowledge, our results are also the first to definitively show the

164   existence of IHR events in mammalian zygotes. Although previous work has suggested the

165   existence of these events, a recent commentary in *bioRxiv* highlights the need for more rigorous

166   analyses to confirm such findings and outlines 3 main points[18]. First, Egli *et al.* argue that

167   because IHR requires physical interaction of the maternal and paternal genomes, there must be a

168   sufficient explanation for how IHR can result from Cas9-mediated DSBs that occur while the

169   maternal and paternal genomes are segregated in separate pronuclei. Second, they suggest that

170   parthenogenesis must be ruled out as a possibility for the observed loss-of-heterozygosity. Last,

171   they suggest that additional measures be taken to rule out the possibility that the observed loss-

172   of-heterozygosity is due to large NHEJ-induced indels emanating from the Cas9 cut site. Our

173   data fulfills all three requirements and further goes on to show that RAD51 is capable of

174   significantly enhancing IHR. With respect to the need for physical proximity between homologs

175   to allow IHR, previous kinetic studies have shown that Cas9 can remain bound to its cut site for

176   up to 6 hours[19], which would be long enough to allow mitotic association of the maternal and

177   paternal alleles in mouse zygotes. Furthermore, an additional study in mouse demonstrated

178   successful correction of a disease mutation in zygotes without the use of exogenous donor

179   DNA[20], supporting the existence of a zygotic IHR mechanism. With regard to the ruling out

180   parthenogenesis, our experimental design relied upon transfer of the paternal mutation to the

181   maternal allele, excluding the possibility of a parthenogenesis-based mechanism. Last,

182   previously published work mouse zygotes showed that the median deletion size associated with a

183   Cas9-induced cut with a single sgRNA was ~10bp, that deletions do not surpass 600bp, and that

184   the occurrence of large deletions (>100bp) was largely sequence-dependent and far too

185   infrequent to account for the high rates of IHR observed in our experiments[10]. In accordance with

186   these findings, our copy-number analyses and F_1 genotyping data rule out large deletions as the

187   source of loss-of-heterozygosity and therefore support our conclusions regarding the existence

188   and enhancement of zygotic IHR.

189   Together, our studies validate the existence of a bona fide IHR-based DSB repair

190   mechanism in the mammalian zygote and demonstrate significant enhancement of this process

191   by the HDR-associated strand exchange factor RAD51. Furthermore, we show that enhancement

192   of the IHR and/or HDR pathways with exogenous RAD51 can be used for highly efficient

193   homozygous KI and donor-free homozygous conversion. Ongoing efforts to generate primate

194   models of human diseases have been hindered by low efficiency, long generation times, and high

195   costs associated with obtaining homozygotes. However, our method has the potential to generate

196   F_0 homozygotes with high efficiency, significantly decreasing costs and study length. Taken as a

197   whole, our findings have broad implications for applications in basic sciences, disease modeling,

198   therapeutic gene editing, and biotechnology.

199

200

201   **<u>Methods</u>**

202   ***Data Availability:*** The raw data supporting the findings in this manuscript can be obtained from

203   the corresponding author upon reasonable request.

204   *Animal Care and Use:* All mouse work was performed with the supervision of the

205   Massachusetts Institute for Technology Division of Comparative Medicine (DCM) under

206   protocol 0416-024-19, which was approved by the Committee for Animal Care (CAC). All

207   procedures were in accordance with the guidelines set forth by the Guide for Care and Use of

208   Laboratory Animals, National Research Council, 1996 (institutional animal assurance no. A-

209   3125-01). All embryos injected for the experiments described in this manuscript were on a

210   C57BL/6NTac background (Taconic; referred to as C57BL/6N in paper).

211   *Preparation of Injection Mixtures*: tracrRNA, crRNAs, and ssODNs were synthesized by

212   Integrated DNA Technologies (see Supplementary Table 1 for sequences). All injection mixtures

213   were prepared in a final volume of 50µL according using the same protocol. Using RNase-free

214   water, reagents, and consumables, crRNA (final concentration 0.61µM), tracrRNA (final

215   concentration 0.61µM), and ultrapure Tris-HCl, pH7.39 (final concentration 10mM,

216   ThermoFisher) were mixed and incubated at 95°C for 5 minutes. The mixtures were cooled to

217   room temperature for 10 minutes on the benchtop and then EnGen Cas9-NLS (New England

218   Biolabs) was added to a final concentration of 30ng/µL. The mixtures were incubated at 37°C for

219   15 minutes before adding any remaining components: ssODN (final concentration 30ng/µL),

220   RAD51 (Creative Biomart, final concentration 10µg/µL). Injection mixtures were stored on ice

221   and briefly heated to 37°C prior to injection. For experiments utilizing RS-1, embryos were

222   cultured in KSOM-AA with 7.5µM RS-1 (Sigma) or DMSO (Sigma, 1:1000) for 24 hours,

223   washed, and cultured in standard FHM until collection for genotyping.

224   *In Vitro Fertilization*: *In vitro* fertilization was performed using FERTIUP® Mouse

225   Preincubation Medium and CARD MEDIA (Kyudo Company) according to the manufacturer's

226   protocol.

227   ***Zygotic Injections:*** Female mice (4-5 weeks old, C57BL/6NJ) were superovulated by IP

228   injection of PMS (5 IU/mouse, three days prior to microinjection) and hCG (5 IU/mouse, 47

229   hours after PMS injection), and paired with males. Plugged females were sacrificed by cervical

230   dislocation at day 0.5pcd and zygotes were collected into 0.1% hyaluronidase/FHM. Zygotes

231   were washed in drops of FHM and cumulus cells were removed. Zygotes were cultured in

232   KSOM-aa medium for one hour and used for microinjection. Pronuclear injection was performed

233   using a micromanipulator (Narishige), microscope (Nikon), and injector (Eppendorf). Zygotes

234   were cultured until collection for genotyping. For experiments giving rise to F_0 animals, embryos

235   were surgically implanted into pseudopregnant CD-1 females (Charles River Laboratories, Strain

236   Code 022) 24 hours post-injection, allowed to develop normally, and recovered following natural

237   birth.

238   ***Embryo DNA Purification***: Embryos were collected at morula stage in 6μL embryo digestion

239   buffer (125μg/mL proteinase K, 100mM Tris-HCl pH 8.0, 100mM KCl, 0.02% gelatin, 0.45%

240   Tween-20, 60μg/mL yeast tRNA) and digested for 1 hour at 56°C. Proteinase K was inactivated

241   via incubation at 95°C for 10 minutes. Embryo DNA was stored at -20°C until use.

242   ***Tail DNA Purification***: Tail snips (~0.5cm length) were collected from animals, placed in 75μL

243   alkaline lysis buffer (25mM NaOH, 0.2mM EDTA), and incubated at 95°C for 30 minutes.

244   Digestion was stopped via addition of 75μL neutralization buffer (40mM Tris-HCl pH 5.0).

245   Samples were stored at 4°C until genotyping.

246   ***$Chd2^{R1684H}$ Genotyping***: Initial PCR was performed using either 3μL embryo DNA or 2μL

247   purified tail DNA. The longer amplification of the nested PCR reaction was performed using the

248   Chd2-RH_Long_F/R primer pair listed in Supplementary Table 2 and an annealing temperature

249   of 65°C. Nested PCR was performed using 2µL of the initial 25µL PCR reaction, the Chd2-

250   RH_F/R primer pair listed in Supplementary Table 2, and an annealing temperature of 65°C.

251   ***Tyr^{C89S} Genotyping:*** Initial PCR was performed using 2µL purified tail DNA. The longer

252   amplification of the nested PCR reaction was performed using the Tyr_Long_F/R primer pair

253   listed in Supplementary Table 2 and an annealing temperature of 65°C. Nested PCR was

254   performed using 2µL of the initial 25µL PCR reaction, the Tyr_F/R primer pair listed in

255   Supplementary Table 2, and an annealing temperature of 65°C.

256   ***Genomic qPCR:*** To determine copy number at specific genomic loci, we developed a strategy

257   utilizing multiplex nested qPCR. We first performed multiplex amplification of both the edited

258   *Chd2* region and a region of the *Gapdh* promoter, which is located on a different chromosome, in

259   a short round of PCR (10 cycles). In the case of our *Shank3B* control experiment, we attempted

260   to match the input DNA concentration used for experiments utilizing DNA from cultured

261   embryos. Based on an estimation of ~6pg DNA per cell and a PCR input of ~30 cells, we used

262   180pg *Shank3B$^{+/+}$* or *Shank3B$^{+/-}$* genomic DNA per initial reaction. We then used the PCR

263   products from the initial multiplex PCR as input for subsequent qPCR using Sso Advanced

264   SYBR Green Supermix (Bio-Rad). qPCR was performed on a CFX96 Touch Real-Time PCR

265   Detection System (Bio-Rad) and analyzed using CFX Maestro software (Bio-Rad). *Chd2* or

266   *Shank3B* signal was normalized to *Gapdh* signal to control for input and a second diploid locus.

267   ***Statistical Analyses:*** Statistical analyses were performed using Prism 6 (Graphpad). For initial

268   experiments in which the effects of RS-1 and RAD51 were unknown, as well as mixed oligo KI

269   experiments where RAD51 could potentially increase either compound heterozygosity or

270   homozygosity, two-tailed analyses were used. All other experiments exploring RAD51's ability

271   to increase KI and homozygous KI efficiencies utilized one-tailed tests. Genomic qPCR

272   performed in Figure 3 was analyzed by unpaired t-test. The graph displays mean±SEM.

273

References

276   1.   Aida, T. *et al.* Cloning-free CRISPR/Cas system facilitates functional cassette knock-in in
277   mice. *Genome Biol* **16,** 87 (2015).
278   2.   Quadros, R. M. *et al.* Easi-CRISPR: a robust method for one-step generation of mice
279   carrying conditional and insertion alleles using long ssDNA donors and CRISPR
280   ribonucleoproteins. *Genome Biol* **18,** 103 (2017).
281   3.   Aida, T. *et al.* Gene cassette knock-in in mammalian cells and zygotes by enhanced
282   MMEJ. *BMC Genomics* **17,** 183 (2016).
283   4.   Yu, C. *et al.* Small Molecules Enhance CRISPR Genome Editing in Pluripotent Stem
284   Cells. *Cell Stem Cell* **16,** 142–147 (2015).
285   5.   Li, G. *et al.* Small molecules enhance CRISPR/Cas9-mediated homology-directed genome
286   editing in primary cells. *Sci. Rep.* **7,** 8943 (2017).
287   6.   Song, J. *et al.* RS-1 enhances CRISPR/Cas9- and TALEN-mediated knock-in efficiency.
288   *Nature Communications* **7,** 10548 (2016).
289   7.   Maruyama, T. *et al.* Increasing the efficiency of precise genome editing with CRISPR-
290   Cas9 by inhibition of nonhomologous end joining. *Nature Biotechnology* **33,** 538–542
291   (2015).
292   8.   Ma, X. *et al.* CRISPR/Cas9-mediated gene manipulation to create single-amino-acid-
293   substituted and floxed mice with a cloning-free method. *Sci. Rep.* **7,** 42244 (2017).
294   9.   Paquet, D. *et al.* Efficient introduction of specific homozygous and heterozygous
295   mutations using CRISPR/Cas9. *Nature* **533,** 125–129 (2016).
296   10.   Shin, H. Y. *et al.* CRISPR/Cas9 targeting events cause complex deletions and insertions at
297   17 sites in the mouse genome. *Nature Communications* **8,** 15464 (2017).
298   11.   Ghodsinejad Kalahroudi, V. *et al.* Two Novel Tyrosinase (TYR) Gene Mutations with
299   Pathogenic Impact on Oculocutaneous Albinism Type 1 (OCA1). *PLoS ONE* **9,** e106656
300   (2014).
301   12.   Takayama, K. *et al.* Highly efficient biallelic genome editing of human ES/iPS cells using
302   a CRISPR/Cas9 or TALEN system. *Nucleic Acids Research* **45,** 5198–5207 (2017).
303   13.   McVey, M. & Lee, S. E. MMEJ repair of double-strand breaks (director's cut): deleted
304   sequences and alternative endings. *Trends in Genetics* **24,** 529–538 (2008).
305   14.   Richardson, C., Moynahan, M. E. & Jasin, M. Double-strand break repair by
306   interchromosomal recombination: suppression of chromosomal translocations. *Genes &*
307   *Development* **12,** 3831–3842 (1998).
308   15.   Moynahan, M. E. & Jasin, M. Loss of heterozygosity induced by a chromosomal double-
309   strand break. *Proc Natl Acad Sci USA* **94,** 8988–8993 (1997).
310   16.   Ma, H. *et al.* Correction of a pathogenic gene mutation in human embryos. *Nature* **548,**
311   413–419 (2017).
312   17.   Peca, J. *et al.* Shank3 mutant mice display autistic-like behaviours and striatal
313   dysfunction. *Nature* **472,** 437–442 (2011).

314   18.   Egli, D., Zuccaro, M., Kosicki, M., Church, G. & Bradley, A. Inter-homologue repair in
315   fertilized human eggs? *bioRxiv* (2017). doi:10.1101/181255
316   19.   Richardson, C. D., Ray, G. J., DeWitt, M. A., Curie, G. L. & Corn, J. E. Enhancing
317   homology-directed genome editing by catalytically active and inactive CRISPR-Cas9
318   using asymmetric donor DNA. *Nature Biotechnology* **34,** 339–344 (2016).
319   20.   Wu, Y. *et al.* Correction of a Genetic Disease in Mouse via Use of CRISPR-Cas9. *Cell*
320   *Stem Cell* **13,** 659–662 (2013).
321

322

Acknowledgements

324

330

Author Contributions

332

333 J.J.W., T.A., M.W., Q.Z., and G.F. designed experiments. J.J.W. and P.Q. performed

334 experiments. J.J.W., T.A., M.W., and G.F. analyzed data. J.J.W., T.A., and G.F. prepared the

335 manuscript.

336

Competing Financial Interests

338 The authors of this manuscript declare no competing financial interests.

339

Materials and Correspondence

341 Correspondence and materials requests should be addressed to G.F. at fengg@mit.edu

342
343

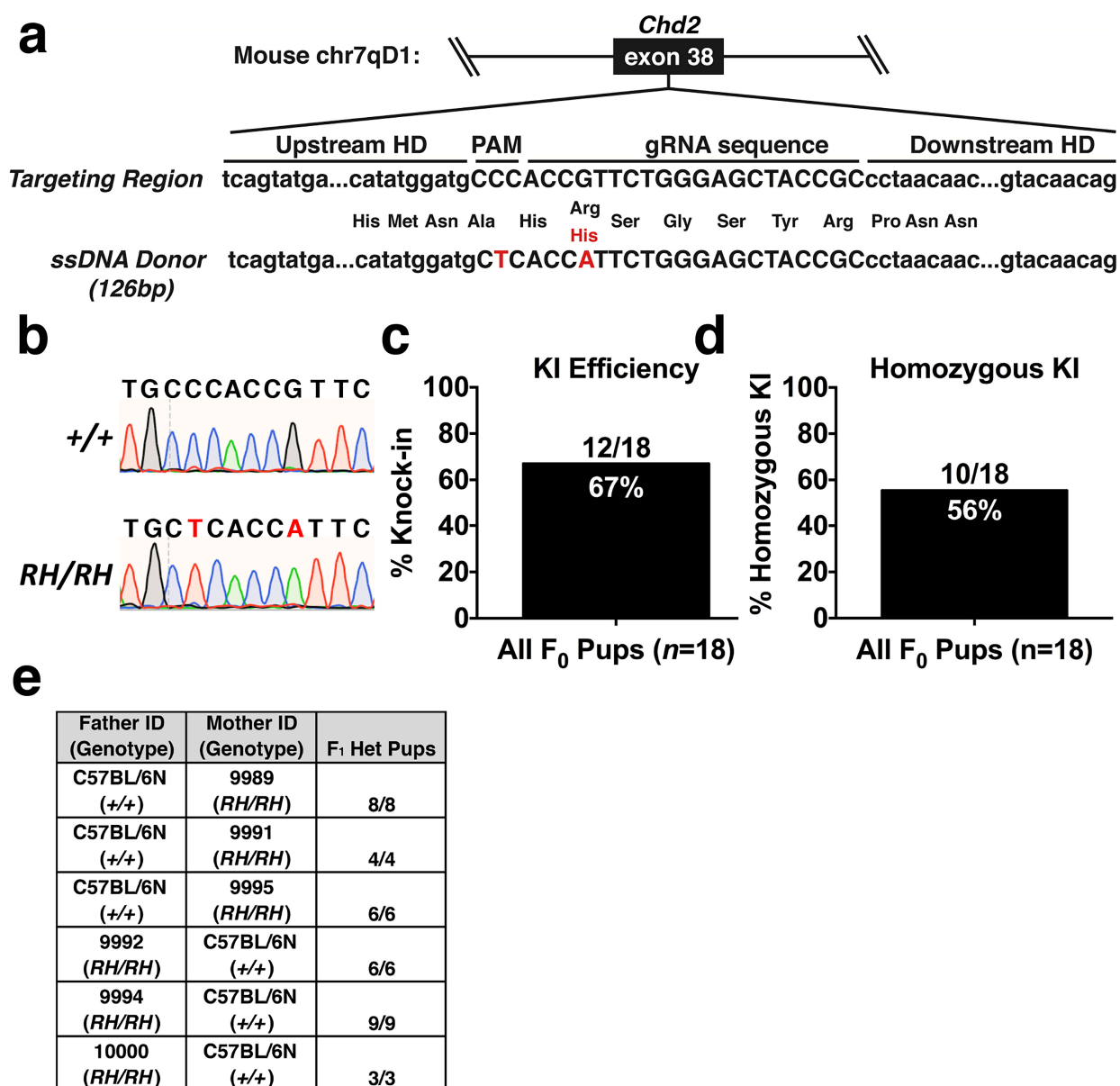**Figure 1: Efficient homozygous knock-in with RAD51. a,** Schematic of the targeting locus and HR donor for generating $Chd2^{R1684H}$ mutant mice. HR donor contains both the c.5051G>A point mutation and a synonymous mutation that destroys the relevant PAM site (HD=homology domain). **b,** Example chromatograms of wildtype (top) and $Chd2^{R1684H/R1684H}$ animals (RH=R1684H). **c,** Overall KI efficiency observed in F_0 pups (pups with ≥1 KI allele/total pups). **d,** Homozygous KI rate observed in F_0 pups. **e,** Genotyping results from F_1 pups derived from crosses between F_0 $Chd2^{R1684H/R1684H}$ animals and wildtype C57BL/6N animals.
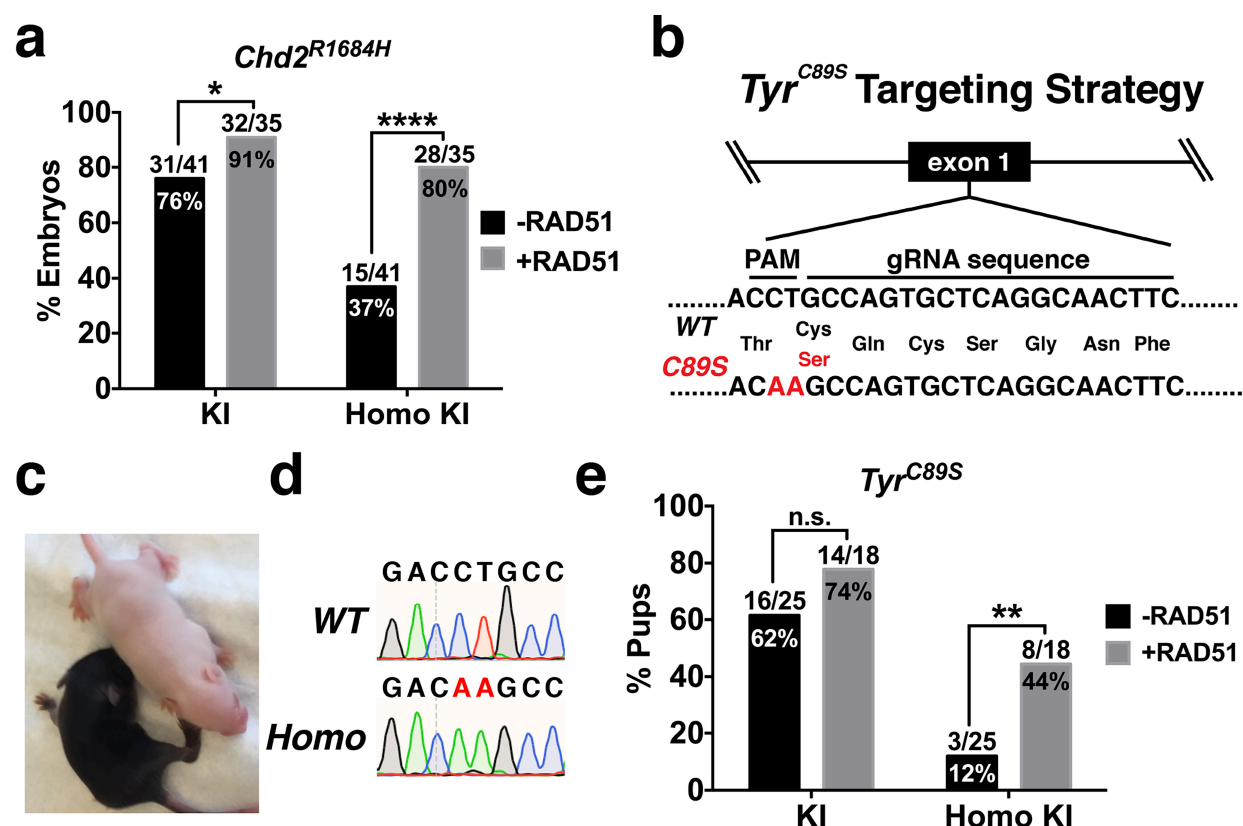
353

Figure 2: Exogenous RAD51 enhances KI efficiency at multiple loci. a, $Chd2^{R1684H}$ PNI using 30ng/µL ssODN with or without RAD51 revealed a slight increase in overall KI efficiency (p<0.05, one-tailed chi-square test) and a dramatic increase in homozygous KI efficiency (p<0.0001, one-tailed chi-square test). **b,** Schematic of knock-in strategy for the albinism-associated Tyr^{C89S} mutation. **c,** Representative examples of $Tyr^{+/+}$ (black) and $Tyr^{C89S/C89S}$ (white) littermates derived from three-component CRISPR injections using exogenous RAD51. **d,** Representative chromatograms from $Tyr^{+/+}$ (top) and $Tyr^{C89S/C89S}$ animals. **e,** Genotyping of F0 animals generated by three-component CRISPR with or without RAD51 showed no significant effect of RAD51 on overall KI efficiency (n.s.=not significant, p=0.166, one-tailed chi-square test), but a significant RAD51-dependent increase in homozygous KI rates (p=0.0081, one-tailed chi-square test).
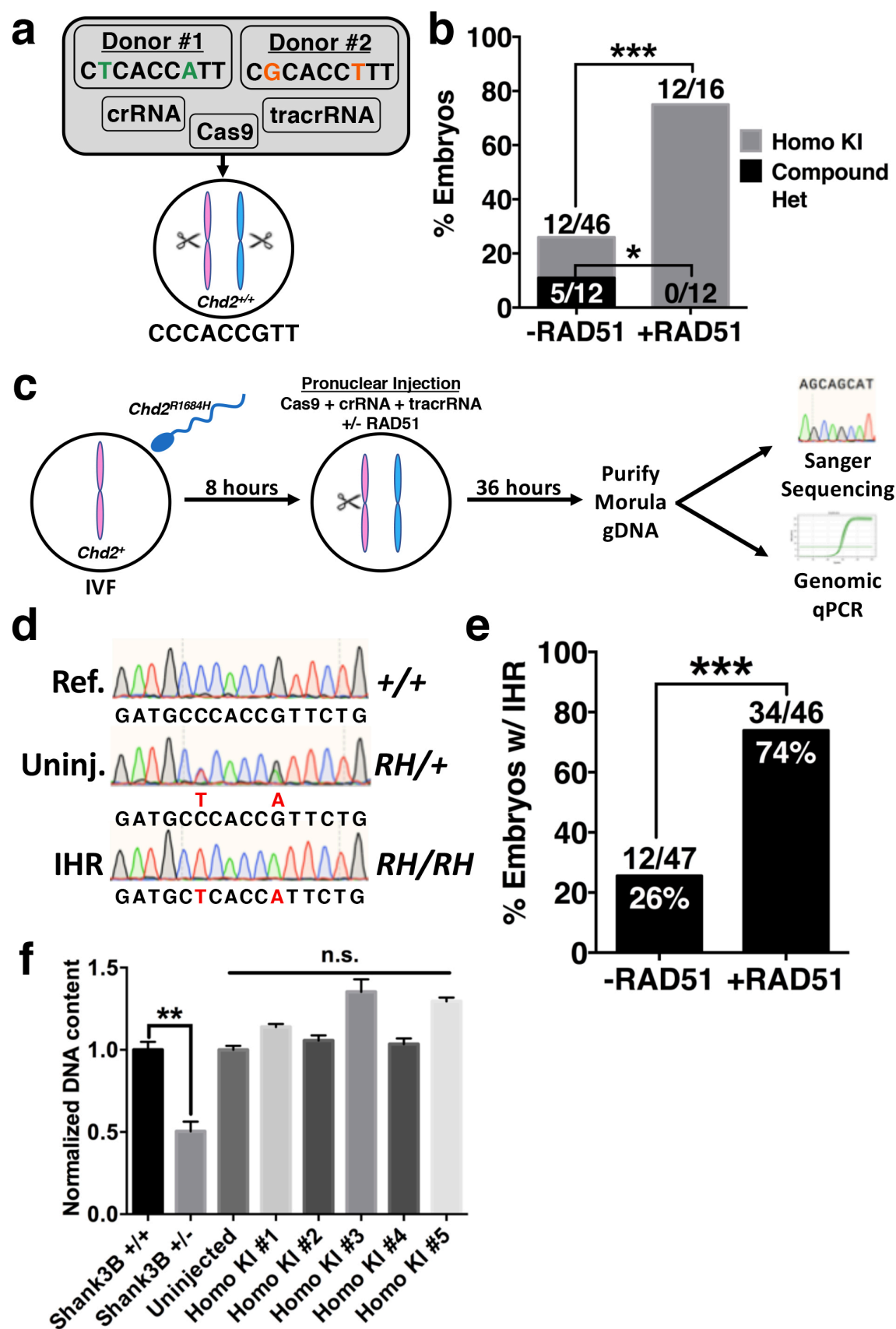
365

366 **Figure 3: RAD51 enhances interhomolog repair. a,** Schematic of strategy to test homozygous

367 KI mechanism. Fertilized embryos were injected with Cas9 protein, crRNA, tracrRNA, and an

368 equimolar mixture of two ssODNs varying by two nucleotides with or without RAD51 protein.

369 **b,** Genotyping results from embryos collected following mixed ssODN injection. Homozygous

370 KI efficiency represents the fraction of homozygous KI events observed in all injected embryos

371 (p=0.0008, one-tailed chi-square test). Compound heterozygous rates represent the fraction of

372 homozygous KI embryos with a different KI event on each allele (p=0.0120, two-tailed chi-

373 square test). **c,** Schematic of strategy for testing RAD51-enhanced IHR. Wildtype C57BL/6N

374 eggs were fertilized *in vitro* by sperm collected from male $Chd2^{R1684H/R1684H}$ mice and cultured

375 for 8 hours. At 8hpf, PNI was performed with Cas9 protein, crRNA, and tracrRNA with or

376 without RAD51 protein. Since *R1684H* mutants carry a mutation in the PAM associated with the

377 crRNA utilized in these experiments, Cas9 is only capable of cutting the maternal allele. Injected

378 embryos were then cultured for 48 hours and collected at morula stage. Half of the purified DNA

379 was used for nested PCR and Sanger sequencing and the other half was used for multiplex PCR

380 and subsequent qPCR to analyze genomic copy number at the *Chd2* editing locus. **d,**

381 Representative chromatograms showing the wildtype reference sequence (Ref., top), an

382 uninjected $Chd2^{R1684H/+}$ embryo generated by IVF (Uninj., middle), and a $Chd2^{R1684H/R1684H}$

383 homozygous mutant (IHR, bottom) generated via donor-free, RAD51-enhanced three-component

384 CRISPR. **e,** Sanger sequencing of IVF-derived embryos revealed a significant increase in IHR in

385 embryos injected with RAD51 (p<0.0001, one-tailed chi-square test). **f,** Genomic qPCR targeting

386 *Shank3B* using 180pg genomic DNA from wildtype and $Shank3B^{+/-}$ mice indicate that our copy-

387 number strategy is capable of identifying heterozygous deletions (lanes 1-2, p=0.00295, unpaired

388 t-test, t=6.47, df=4, *n*=3 technical replicates per sample, error bars=SEM). qPCR using DNA

389 from an uninjected embryo and 5 randomly selected homozygous $Chd2^{R1684H}$ embryos revealed

390 normal copy number at the *Chd2* editing locus in all animals (lanes 3-8, p>0.05, unpaired t-test,

391 t=4.60, df=6, *n=4* technical replicates per sample, error bars=SEM)**.**